New Methods for Measuring Impact Force on a Flexible Barrier from Rockfall and Debris Flow based on Large-scale Flume Tests

by

Dao-Yuan TAN, PhD

(Research Assistant Professor and Corresponding Author)
Department of Civil and Environmental Engineering
The Hong Kong Polytechnic University, Hung Hom, Kowloon, Hong Kong, China
Email: dytan@polyu.edu.hk

Jian-Hua YIN, Chair Professor
Department of Civil and Environmental Engineering
The Hong Kong Polytechnic University, Hung Hom, Kowloon, Hong Kong, China
Tel: (852) 2766-6065, Fax: (852) 2334-6389, Email: cejhyin@polyu.edu.hk

Wei-Qiang FENG, PhD
(Assistant Professor)
Department of Ocean Science and Engineering,
Southern University of Science and Technology, Shenzhen, 518055, China
Email: fengwq@sustech.edu.cn

Jie-Qiong QIN, PhD
Department of Civil and Environmental Engineering
The Hong Kong Polytechnic University, Hung Hom, Kowloon, Hong Kong, China
Email: jieqiong.qin@connect.polyu.hk

and

Zhuo-Hui ZHU, PhD
Department of Civil and Environmental Engineering
The Hong Kong Polytechnic University, Hung Hom, Kowloon, Hong Kong, China
Email: zhuo-hui.zhu@connect.polyu.hk

Manuscript submitted to *Engineering Geology* for possible publication as a research paper

October 2020

Abstract: Accurate determination of impact loads is of great necessity for safe and economical design of flexible barriers. Nevertheless, measurement of the impact force on a flexible barrier is still an open problem due to the highly deformable flexible net under impact and stress concentration on force transducers. In this study, large-scale physical modelling with new design of instrumentation was adopted to validate and optimise existing methods for measuring the impact forces on a flexible barrier. Specifically, single-boulder impact tests were conducted to verify the accuracy of those methods. A debris flow impact test was performed to quantitatively investigate the dynamic behaviour of a flexible barrier under the impact of a debris flow. Thanks to the well-designed instrumentation, the impact force distribution characteristics of a debris flow on a flexible barrier is discovered. During the interaction process, the debris flow first impacted on the bottom area of the flexible net, then the dynamic impact moved up with gradual deposition of debris material. It is found that the impact pressure on the central area is much larger than that on two sides. Therefore, triangular-shaped load distribution is used to optimise the simple method for measuring the impact force induced by a debris flow. Attributable to the good accuracy and simple instrumentation requirement, this new simple method can be generalized for real-time monitoring of impacts on flexible barriers installed in natural terrains.

Keywords: Rockfall; Debris flow; Impact force measurement; Large-scale flume test

1. Introduction

Rockfall and debris flow are common natural hazards in mountain areas (Su et al .2017; Cui *et al.* 2018; Kattel et al. 2018; Liu et al. 2020). In spite of their limited volumes compared to deep-seated landslides, they can be destructive and cause catastrophic damages to buildings and infrastructure in the influenced areas due to the high bulk density and large front velocities (Bugnion and Wendeler 2010; Jakob *et al.* 2012; Peng et al. 2015). Appropriate countermeasures are required for rockfalls and debris flows due to the high frequency and difficulty of prediction (Takahashi 2014). For safe and economical design of mitigation systems, accurate determination of impact load on the resisting structures is of great necessity. Flexible barriers were firstly commercially developed by Brugg in the 1970s to halt large boulders (Kane *et al.* 1993; Hearn *et al.* 1995). Recently, this countermeasure is regarded as a potential solution for controlling other geohazards such as granular avalanches (Ashwood and Hungr 2016; Xiao et al. 2020) and debris flows (Leonardi et al. 2016; Kwan *et al.* 2014; Volkwein 2014). A typical flexible barrier usually consists four components: a flexible ring net, supporting posts holding the ring net, strand cables and foundations supporting the posts. The impact force on a flexible barrier is difficult to be directly measured by installing pressure transducers in the interception structure (*e.g.* flexible mesh nets or flexible ring nets) because of two reasons: (a) Installation of pressure transducers in the flexible net will unavoidably weaken the capability of large deformation, which is one major advantage of flexible barriers for reducing the impact forces from boulders and debris flows; (b) Stiffness difference between the rigid measurement surface of the pressure transducer and the deformable flexible barrier also leads to stress concentration on the transducer and over-estimation of the impact force. Therefore, indirect measurement methods are normally applied to detect the impact force from the responses of the components of a flexible barrier.

Tensile forces in the horizontal ropes for reinforcing the flexible net have been measured and utilised for estimating the impact load from a debris flow. Song *et al.* (2017) measured the tensile forces in the horizontal cables of a flexible barrier impacted by granular flows in a centrifuge model and back calculated the impact force considering the maximum deflection of the barrier. Wendeler *et al.* (2019)

measured the tensile forces in the horizontal cables of a full-scale flexible barrier during a debris flow event and utilised the forces to develop a new load model for impact force calculation. Besides, the tensile forces in the supporting cables have been utilised to quantify the impact force on the supporting structures of a flexible barrier. Denatale *et al.* (1999) conducted large-scale physical modelling experiments for testing the performance of flexible barriers supported by posts and cables. From the results of those tests, they found that flexible barriers can efficiently mitigate small debris flows. Tensile forces in the supporting cables were measured by load cells installed between cables and the ground anchors. Although, the total impact forces were not measured in that study, they found that the peak loads in the supporting cables occurred at the same time with the maximum momentum impulse to the net, which indicates that the maximum tensile forces on the supporting cables can be used to reflect the impact behaviour of a debris flow on a flexible barrier. Bugnion and Wendeler (2010) conducted full-scale shallow landslide impact tests and measured tensile forces in the supporting cables. Based on the peak tensile forces, an equation was established to calculate the maximum dynamic impact pressure induced by a shallow landslide. Results of the previous research prove that the tensile forces in the supporting cables can quantitatively reflect the dynamic response of a flexible barrier impacted by a debris flow.

Based on the findings from relevant research, those existing methods have been successfully utilised to investigate the impact of a debris flow against a flexible barrier by measuring tensile forces in major supporting structures (ropes reinforcing the net or cables supporting the posts). However, those existing methods may not be able to realistically quantify the magnitude of the impact force because the force can be reduced by the large deformation of the flexible net. Brighenti et al. (2013; 2015) proposed a simplified analytical model based on the equation of equilibrium of wires under large displacement conditions for estimating the restraining forces and the cable stresses, which has good performance compared with parametric analysis and full-scale tests. Tan *et al.* (2018b) proposed a novel method to directly measure the impact force on the flexible net based on the tensile forces within the flexible net. This method has been utilised for monitoring the dynamic response of a flexible barrier under the

impacts of rock boulders (Tan *et al.* 2018b) and dry granular flows (Tan *et al.* 2018a). However, applicability and accuracy of those methods should be further validated using appropriate methods and reliable experiment data before the practical application.

This study aims to verify the existing methods and develop appropriate methods for accurate measurement of the impacts from falling boulders or debris flows and efficient monitoring of the dynamic response of full-scale flexible barriers installed in natural slopes and gullies. First, the data of two large-scale boulder impact tests using single boulders with the diameters of 400 mm and 600 mm, as shown in Tan et al. (2018b), are utilised to verify the simple methods. With the well-designed instrumentation in the flexible barrier, the forces in different components during the interaction with the moving boulder were measured. The impact force from the boulder, as a reference for verification of the existing methods, is back calculated by tracking the movement of the boulder. Afterwards, a large-scale debris flow impact test was performed to quantitatively investigate the impact behaviour of a debris flow on a flexible barrier. The characteristics of the impact pressure distribution in the flexible net are discovered with the help of the sophisticated instrumentation. By adopting the experiment data and findings, a new simple method that can feasibly detect the impact force from a debris flow is developed by measuring the tensile force in the outline cable, which can be generalized for real-time monitoring of impacts on flexible barriers installed in natural terrains attributable to the acceptable accuracy and simple instrumentation requirement.

2. Experimental setup and procedure

2.1 Experimental setup

A large-scale experiment facility for performing boulder and debris flow impact tests was constructed in the Road Research Lab of the Hong Kong Polytechnic University. The view of the facility is illustrated in Figure 1. This facility is comprised of three major components: (i) a 7-m-long, 1.5-m-wide and 33-degree-inclined flume, (ii) a 4-m^3-capacity material container located at the upstream of the

flume, and (iii) an instrumented prototype flexible barrier located at the downstream of the flume. The side walls of the flume are made up of transparent tempered glass for clear observation of the movement of the impacting boulder or debris flow. A flip-up door facing to the flume is installed in the front wall of the container to release a rockfall or initiate a debris flow. A patented door-opening system is utilised to assist the door opening process for initiating debris flows uniformly and quickly (Tan *et al.* 2020). The prototype flexible barrier at the lower end of the flume consists of steel wire rings (No. ROCCO 7/3/300, GEOBRUGG) with the diameter of 300 mm, which has been commonly used for rockfall and debris flow mitigation (Sze et al 2018). Those steel wire rings are spread by a rectangular-shaped outline cable. The outline cable is stretched by two steel posts hinged to the ground, which can rotate in the plane of impact. Each post is supported by two strand cables, as shown in Figure 2.

2.2 Instrumentation

As the main research object, the flexible barrier is well instrumented to investigate the dynamic behaviour under impacts. Detailed instrumentation of the flexible barrier is shown in Figure 2. Corresponding to the major components of a flexible barrier: a flexible ring net, an outline cable, and supporting structures, three types of transducers are installed in the flexible barrier for measuring the forces in different components: (i) mini tension link transducers between rings in the flexible net, (ii) a tension link transducer in the outline cable, and (iii) high capacity tension link transducers in the supporting cables. Besides, a high-speed camera (MotionBLITZ Cube, MIKROTRON, Eching, Germany) with the set recording speed of 500 fps and resolution of 1024×768 pixels is located at the right side of the flexible net to capture the velocity of the impacting boulder, the front velocity of the debris flow, and the deformation profile of the flexible net during impact. The mini tension link transducers within the flexible net are designed and developed as connectors linking adjacent net rings. As described in Qin et al. (2020), this transducer has a sensing element and a protection tube. The sensing element is a 316 stainless bar (40 mm long, 20 mm wide, and 10 mm thick) with two U-shaped openings at both ends for rings connection. The sensing element is manufactured by computer numerical control (CNC) machining technology to ensure the integrity and performance. An FBG

sensor is attached to the surface of the sensing bar at its central axis by epoxy adhesive for tensile force measurement. All transducers utilized in this study have been calibrated in the soil laboratory of the Hong Kong Polytechnic University. To measure the impact loading distribution on the flexible net, individual areas composed of interwoven rings are separated from the main net and reconnected to the neighbouring rings by mini-tension link transducers. Due to the diverse impact characteristics of a falling boulder (concentrated impact force) and a debris flow (distributed impact pressure), the arrangement of transducers in the flexible net for boulder impact tests and debris flow impact tests are adjusted correspondingly. Figure 3 presents the arrangements of the mini-tension link transducers in the flexible nets for the boulder (Figure 3a) and debris flow impact tests (Figure 3b). In the supporting strand cables, bridge-based tension link transducers with the certified capacity of 50 kN are installed at the joints between the cables and the foundation. Those transducers are connected to a data-logger（NI PXIe-1082, National Instruments, Austin, U.S.A.), which is capable of recording 48 transducers at 1000 Hz simultaneously. Light yellow alert tapes are attached to the post and the flume as the reference scale.

2.3 Source materials and test procedure

Two boulder impact tests, referring to Tan et al. (2018b), and one debris flow impact test were performed using the large-scale physical modelling facility. Granite boulders with the diameters of 400 mm and 600 mm were prepared to generate staged impact forces (see Figure 4a). For the boulder impact tests, a boulder was lifted into the upstream material container. For the debris flow impact test, nearly 2 m^3 of fully saturated debris material was prepared in the material container with the water content of 52.74%. The debris material was prepared by mixing Completely Decomposed Granite (CDG) and aggregate with water using an electronic soil mixer before being poured into the reservoir. The content of coarse particles (diameter larger than 10 mm) of the debris material used in the test was managed referring to the Tsing Shan debris flow in Hong Kong (King 2013) to reflect the particle size distribution (PSD) characteristics in a real debris flow event. As a comparison, the representative PSD curves of the debris material used in this study and the material of the Tsing Shan debris flow are plotted in Fig 4b. Once the material had been placed in the container, the test was started by rapidly flipping the front

door to initiate a rockfall or a debris flow. Data from the transducers in the flexible barrier were measured and stored in the datalogger. Continuous photos were taken by the side-view high-speed camera for interaction and movement analysis.

3. Verification of methods for impact force measurement

3.1 Back calculation of impact force

A method is proposed to back calculate the impact force induced by a boulder based on the momentum conservation law. By tracking the location of the boulder from continuous photographs taken by the high-speed camera, the movement trajectory of the boulder during impact can be captured. Taking the time interval between two continuous photographs as the denominator, velocity change of the boulder during the impact process can be obtained. Figure 5 shows the movement trajectory and the velocity component in the impact direction of the boulder in the tests.

Following the momentum conservation law, the impact impulse on the flexible barrier is originated from momentum change of the boulder:

$$F \cdot \Delta t = m \cdot \Delta v \tag{1}$$

where F is the impact force; m is the mass of the moving object; and Δv is the velocity change at the time period Δt.

By obtaining the moving distance in a specific small time interval (dt) from the movement trajectory of the boulder, the average velocity in the time interval can be calculated. Therefore, the impact force from the boulder in the *i-th* time interval (dt_i) can be calculated using the following equation:

$$F_i = \frac{m \cdot \Delta v_i}{dt_i} \tag{2}$$

where F_i and Δv_i are the impact force and the velocity change in the *i-th* time interval, respectively.

Therefore, the impact force of a boulder can be back calculated by tracking its movement during the impact process. Figure 6 illustrates the impact force induced by the boulder and the measured tensile force in the outline cable in the boulder impact tests, where an identical trend was observed in both tests. The good consistency shows that the impact induced by the boulder can be feasibly reflected by the dynamic response of the flexible net. The calculated peak impact force is therefore used to verify the accuracy of the existing methods. Nonetheless, the impact forces measured from the continuous photographs show fluctuated trends, as observed in Figure 6(i). This is mainly because the displacement measured from the photograph analysis cannot describe the movement precisely enough for a smooth curve of its second derivation (that leads to acceleration and force). The accuracy of this method could be improved with the help of the advanced technology by embedding an accelerometer in the rock boulder (Niklaus et al. 2017).

3.2 Methods for measurement of impact force

Measurement of impact force by tensile forces in horizontal outline cables

Song *et al.* (2017) performed a series of centrifuge tests using different geophysical flows impacting on a flexible barrier, which was simulated by a rubber membrane reinforced by four horizontal cables at different heights to restrict the deformation of the membrane and carry impact forces. Two rigid posts were installed to support the membrane and horizontal cables. In that study, a simple method was proposed for measuring the impact force from a geophysical flow based on the tensile forces in the horizontal cables. That method simplified the 3D impact surface of a flexible barrier into a 2D curve of the horizontal cable and assumed that the impact load was uniformly distributed along the cable. The impact force was calculated by decomposing the tensile force in the horizontal cable (T) into a normal component (T_n) and a horizontal component (T_h) to the barrier surface, as shown in Figure 7. The normal

force component was regarded as the impact load induced by the impacting mass. Therefore, the total impact force can be calculated by summarising the normal component of the tensile forces in all horizontal cables:

$$F_{impact,cable} = \sum_{i=1}^{n} 2\mathrm{T}_i \cos\varphi_i \quad (3)$$

where $F_{impact,cable}$ is the calculated impact force based on the tensile forces in the horizontal cables; n is the total number of horizontal cables; T_i is the tensile force in the i_{th} horizontal cable; and φ_i is the deflection angle of the i_{th} horizontal cable.

For the prototype flexible barrier used in this study where the flexible net is stretched by the outline cable, as shown in Figure 3, the upper and lower outline cables can be regarded as the horizontal cables which can transfer the impact force on the flexible net to the supporting structures. Therefore, the measured tensile force in the outline cable is used to estimate the impact force from a boulder using Eq. 3. Even the deflection of the flexible net can reach nearly 1 m due to the high flexibility of the flexible net, as observed in the boulder impact tests in Figure 5, the deformation of the outline was almost negligible. Therefore, the deflection angle (φ) of the outline cable is regarded as 0, and the total tensile force (T) is used to calculate the impact force with reasonable conservation. By ignoring the friction between the outline cable and the supporting posts, the tensile forces in the upper and the lower cables are regarded as the same. It should be noticed that the outline cable used in this study forms a loop surrounding and supporting the flexible net, where the tensile force can be transferred from the upper cable to the lower cable by the internal force balance. For the field flexible barriers, where the upper and the lower cables are independent, this assumption is unrealistic, especially for debris flow impact. The calculated impact forces using this method are listed in Table 1.

Measurement of impact force by tensile forces in supporting cables

In this study, a typical flexible barrier for rockfall and debris flow mitigation in open hillside was assembled for investigating the dynamic responses of different barrier components during impact. For a flexible barrier installed in a natural slope, the net is normally stretched by a series of steel posts, and each post is supported by strand cables connected to anchors and foundations (Sze *et al.* 2018; Volkwein 2014; Kwan *et al.* 2014). The arrangement of the supporting structures of the studied flexible barrier is shown in Figure 8. An analytical solution has been derived by decomposing the tensile forces in the supporting cables. Without any simplification, this solution can precisely determine the impact force on the supporting structures. Summary of the components of the tensile forces in the impact direction gives the total impact force on the supporting structures, which can be calculated as:

$$F_{impact,supporting} = \frac{l_{post}}{l_{impact}}\left[(F_{BL} + F_{BR}) \cdot \cos\delta \cdot \cos\beta - (F_{AL} + F_{AR}) \cdot \cos\gamma \cdot \cos\alpha\right] \quad (4)$$

where $F_{impact,supporting}$ is the impact force calculated from the tensile forces in the supporting cables; l_{post} is the distance between the rotation fulcrum of the post and the connecting point of the cables; l_{impact} is the distance between the rotation fulcrum of the post and the point of application of the impact force; α, β, γ, δ are the corresponding included angles of the supporting cables, which are 76°, 60°, 62°, 24°, respectively; F_{AL}, F_{AR}, F_{BL}, and F_{BR} are the measured maximum tensile forces in the supporting cables, as listed in Figure 9. The calculated impact forces using Eq. 4 are listed in Table 1 for comparison.

Measurement of impact force by tensile forces within flexible net

The basic principle of this method has been described in Tan *et al.* (2018b). Generally, the measurement area is separated from the main net and reconnected to neighbouring rings by mini tension link transducers (see Figure 3). By assuming that the deformation of the flexible net in the measured area is a symmetrical cone, the impact force can be calculated from the summary of the tensile forces of the transducers in the measurement area:

$$F_{impact,net} = \cos\frac{\theta}{2}\sum_{i=1}^{n} T'_{ring,i} \quad (5)$$

where n is the total number of the transducers linking the separated net for measurement to the main net; θ is the included angle of the impacted flexible net, which can be measured from the photograph taken by the high-speed camera at the moment of the largest deformation; and $T'_{ring,i}$ is the orthogonalized tensile force measured by the *i-th* mini-tension link transducer. Orthogonalization should be processed before utilization of the tensile forces because some transducers were not directing to the cone centre due to the interwoven structure of the flexible ring net.

Two simplifications have been made for adoption of this method. The first assumption is that the deformation of the flexible net in the measurement area is assumed cone symmetric. The second assumption is that the peak loadings of all mini-tension link transducers occur at the same time. Therefore, verification is required to quantify the effects of the simplifications on the accuracy of this method. The peak forces of all mini-tension link transducers and the included angle of the flexible net are presented in Figure 9 for calculation of the impact force using Eq. 5. The calculation results are listed in Table 1.

Verification of the methods

The impact forces induced by the boulders and the calculated impact forces using the above-mentioned methods are listed in Table 1. The relative errors of those methods are also calculated for comparison and verification. It can be found that the method based on the tensile forces in the horizontal cables underestimates the impact forces in the boulder impact tests. This is mainly due to two reasons: First, the impact force reduced by the deformation of the flexible net cannot be quantified using this method when the mass of the net is unneglectable to that of a boulder or a debris flow; Second, the impact load induced by the boulder is a concentrated force, which normally cannot be directly imposed on the horizontal cables. Therefore, this method cannot accurately calculate the impact force from a boulder. For quantifying the impact force from a debris flow, the accuracy of this method will be further verified in the following section. The analytical solution for calculation of the impact force on the supporting

structures underestimates 31.9% and 37.2% of the impact forces of the boulders with the diameters of 400 mm and 600 mm. The similar reduction ratios of the impact forces in both boulder impact tests indicate that the deformation of the flexible net can reduce a part of the impact force (around 35% based on the comparison results in this study), which is consistent with the findings in the literature (Wendeler *et al.* 2019; Ashwood and Hungr 2016). The method based on the tensile forces within the flexible net accurately predicts the impact force of the 400-mm boulder and 14% underestimates the impact force of the 600-mm boulder. The good consistency between the calculation results and the measured forces in both boulder impact tests verifies the accuracy of this method.

4. Investigation of impact from a debris flow on a flexible barrier

4.1 Impact characteristics of a debris flow on a flexible barrier

A large-scale debris flow impact test was performed to study the dynamic response of a flexible barrier and develop appropriate methods to simply and accurately measure the impact force from a debris flow. To better understand the impact pressure distribution in the flexible net, 13 mini-tension link transducers were installed in the flexible barrier. The arrangement of those transducers is plotted in Figure 3(b). The tensile force histories of all mini-tension link transducers installed in the flexible ring net and the outline cable in the debris flow test are presented in Figure 10. By selecting typical time points based on the force history of the mini-tension link transducer in the outline cable (transducer 13 in Figure 10), the force distributions within the flexible net at different impact stages are shown by contours in Figure 11. The contours are generated by interpolating the forces measured by all tension links installed in the flexible barrier. These contours are used to visualize the characteristics of the impact pressure distribution other than realistically represent the impact pressure on the rings. From those contours, it can be observed that the debris flow firstly impacted on the bottom central area of the flexible barrier at 0.255 s. With gradual deposition of the debris material, the impact area of the dynamic loading on the flexible barrier moved up and reached the maximum value at 0.350 s. After the dynamic impact, the static pressure of the debris deposition mainly acted on the upper central area of the flexible barrier.

From the series of contours, it can be concluded that the impact pressure on the central area is much larger than which on two sides instead of being uniformly distributed on the flexible barrier, which fits well with the conclusion drawn by Wendeler *et al.* (2019) from back calculation using the data of field-scale debris flow impact tests. Figure 12 shows that the tensile forces in the supporting cables have identical trends with the tensile force in the outline cable.

4.2 Development of simple method for measuring impact force of debris flow

Since the impact force from a debris flow cannot be calculated by tracking its movement as the method adopted in the boulder impact tests, the method for measuring the impact force using the tensile forces between net rings, which has been verified by the data of the boulder impact tests, is applied to quantify the impact force of a debris flow. From the force histories of the mini-tension link transducers in Figure 10, the peak loadings of all transducers in the flexible net are obtained and shown in Figure 13. It can be observed from the growth of the impact pressure in Figure 11 and the distribution of the peak forces in the flexible net (see Figure 13a) that the impact load was mainly imposed on the central area, thus the peak tensile forces of the mini-tension link transducers in the central area (Transducers 1-8) are used to calculate the impact force using Eq. 5. The calculation result is used to validate the accuracy of other simple methods for estimating the impact force from a debris flow. The photograph representing the largest deformation of the flexible barrier is shown in Figure 13(b). It is worth noting that the deflection of the outline cable is negligible compared to the maximum deflection of the flexible net. By obtaining the required parameters from Figs. 12 and 13(b), the calculation results using Eq. 3 and Eq. 4 are listed in Table 2. It is found that the impact force on the supporting structures is 31.4% less than the impact force on the flexible net, which further proves that the flexible barrier can reduce a certain percentage (higher than 30%) of the impact force by the large deformation of the flexible net. On the other hand, the simple method based on the tensile force in the outline cable obviously overestimates the impact force when adopting the assumption that the impact load is uniformly distributed along the cable. However, based on the discovered force distribution characteristics in the flexible net, it is found that the impact pressure on the central area is much larger than which on two sides. Therefore, it is more

rigorous to assume that the impact load distribution along the outline cable is isosceles triangular-shaped other than rectangular-shaped, and the original simple method (Eq. 3) can be optimised as:

$$F_{impact,outline} = \frac{1}{2}\sum_{i=1}^{n} 2T_i \cos\varphi_i \tag{6}$$

From the comparison results in Table 2, it is illustrated that the optimised simple method can be used to measure the impact force of a debris flow on a flexible barrier with an acceptable relative error of 17.9%.

5. Discussion

In this study, the continuous photographs taken in the short impact period by high-speed camera were used to measure the velocity change of boulders during impact. This method has been proved with an overall acceptable accuracy (Bourdonnaye et al. 2012; Park et al. 2013). However, determination of the physical scale in photos and spatial relationship between the lens and the measured object may add errors to this method. The changing location of the boulder during impact and the discontinuity of the photographs may underestimate the velocities of the boulder. Corresponding measures have been taken in this study to increase the accuracy: (a) the rock boulders have known diameter and good sphericity, which can be used as reference for determining the physical scale and location of the boulder in the photographs; (b) the camera has been set carefully to be perpendicular to the measured target. Recently, researchers have adopted many state-of-the-art approaches in large-scale rockfall and debris flow impact tests for accurate and reliable data acquisition, which provides good references to our future study: measuring the acceleration of a impacting boulder by an embedded accelerometer (Niklaus et al. 2017; Volkwein and Klette 2014), measuring the impact pressures of debris flows by pressure transducers on the slope (Bugnion et al. 2012), measuring loads on post foundations (Volkwein et al. 2016), measuring tensile forces in posts and anchors (Platzer et al. 2020), and measuring the total retention forces directly (Wendeler et al. 2019).

Three methods are listed in this study for impact force determination: force on the supporting structures (represented by Eq.4), force on the flexible net (represented by Eq. 5), and force on the outline cables (represented by Eq. 6). Eq. 4 provides a theoretical solution for calculating the impact force on the supporting cables, which is easy to be measured, quantified and has been widely applied in centrifuge modeling tests (Song. et al .2019) and field-scale flexible barrier tests (Wendeler et al. 2007). Eq. 5 is an original method proposed in Tan et al. (2018b) for direct measurement of the impact force on the flexible net, which is larger than the impact force on the supporting structures. This method has been verified by large-scale boulder impact tests and utilized to validate the simple methods. Even through, this method was originally proposed for calculating the concentrated impact of boulder. It can be found from the load distribution in Figure 11 that even the debris flow has a width equal to the flume (1.35 m in this study), the major impact pressure is imposed on the central area of the barrier. Therefore, Eq. 5 may slightly underestimate the distributed impact force of a debris flow. Moreover, this method assumes that the peak loadings of all mini-tension link transducers occur at the same time, which overestimates the impact loads. Eq. 6 is a simple method for impact force estimation based on the tensile force on the outline cable, while similar methods have been proposed by Song et al. (2018) and Wendeler et al. (2019). A triangle distribution of impact loads on the flexible barrier has been observed in large-scale flume tests and utilized to optimize this method. Eq. 6 has also been validated by large-scale debris flow flume tests with acceptable accuracy.

6. Conclusions

Accurate determination of the impact loads from rockfall or debris flow is of great importance for design and maintenance of flexible barriers, which has raised much attention from researchers. Methods for measuring impact forces have been developed in this study using large-scale physical modelling. The data of two boulder impact tests and a debris flow impact test were utilised to verify and optimise the accuracy and applicability of those methods. Major conclusions of this study are summarised as follows:

(a) The method based on the tensile forces in the flexible net can accurately measure the maximum impact force from a boulder with the help of the well-designed instrumentation in the large-scale physical modelling experiments.

(b) The method based on the tensile force in the outline cable significantly underestimated the concentrated impact load in the boulder impact tests because the impact force from a single boulder is normally imposed on the flexible net rather than directly on the reinforcing cables.

(c) The measured impact force in the supporting structures was almost 35% less than the impact force induced by the boulder in the boulder impact tests and 31% less than the force induced by a debris flow in the debris flow impact test. The attenuation of the peak impact forces shows that the flexible net can reduce a certain percentage of the impact load before it is transferred to the supporting structures, and the force reduction ratio can be used to quantify the efficiency of flexibility of a flexible net in reducing impact loads.

(d) The pressure induced by the debris flow during the impact process was visualised by a series of contours. During the interaction, the debris flow firstly impacted on the central bottom area of the flexible barrier, then the impact area rose up with the gradual deposition of the debris material. It can be observed that the pressure on the central area of the flexible barrier was much larger than the pressures on two sides, and the load distribution along the barrier can be simplified as an isosceles triangle.

(e) The simple method based on the tensile force in the outline cable obviously overestimated the impact force from a debris flow because of the unrealistic assumption of the uniformly distributed impact load along the horizontal cable. Based on the load distribution characteristics discovered in this study, the simple method was optimised by adopting the isosceles triangle-shaped load distribution along the barrier. With this optimization, the accuracy of the simple method can be significantly improved.

From the findings in this study, the method based on the tensile forces in the flexible net can accurately measure the impact force on a flexible barrier. Even though, this method requires relatively

sophisticated instrumentation in the flexible barrier. In the boulder impact test, a high-speed camera and 10 self-invented mini-tension link transducers were installed for the application of this method. Therefore, this method is more appropriate for the purpose of accurate measurement of the impact force on a flexible barrier in large-scale physical modelling study. For the practical application, the optimised simple method using the tensile force in the outline cable is suggested to be generalized for monitoring of the dynamic response of flexible barriers installed in natural terrains, which has satisfactory accuracy and good adaptability considering the simple instrumentation requirement and easily obtainable parameters. The findings in this study are based on a series of large-scale tests using a flexible barrier with strand wire ring net (interlaced rings with the diameter of 300mm), and the impact behaviour of other types of nets such as wire mesh nets and spiral rope nets should be further studied by conducting more relevant tests. Even though, this study provides a valuable reference to the study of flexible protection system for rockfall and shallow landslide prevention.

Acknowledgement

The work in this paper is supported by a Collaborative Research Fund project (Grant No.: PolyU 12/CRF/13E), a Research Impact Fund project (R5037-18)，three General Research Fund projects (PolyU 152796/16E, PolyU 152209/17E; PolyU 152130/19E) from Research Grants Council (RGC) of Hong Kong Special Administrative Region Government (HKSARG) of China. The authors also acknowledge the financial supports from Research Institute for Sustainable Urban Development of The Hong Kong Polytechnic University (PolyU), Center for Urban Geohazard and Mitigation of Faculty of Construction and Environment of PolyU, and grants (BBAG, ZVNC, RBCN, ZDBS) from PolyU.

References

A. de La Bourdonnaye, A., Doskočil, R., Křivánek, V., and Štefek, A. (2012). Practical experience with distance measurement based on single visual camera. *Advances in Military Technology*, 7(2), 49-56.

Ashwood, W., and Hungr, O. (2016). Estimating total resisting force in flexible barrier impacted by a granular avalanche using physical and numerical modeling. *Canadian Geotechnical Journal*, 53(10), 1700-1717.

Brighenti, R., Segalini, A., and Ferrero, A. M. (2013). Debris flow hazard mitigation: a simplified analytical model for the design of flexible barriers. *Computers and Geotechnics*, 54, 1-15.

Brighenti, R., Ferrero, A. M., Segalini, A., and Umili, G. (2015). Study on the mechanical behaviour of flexible barriers by in situ testing and modelling. In *Engineering Geology for Society and Territory*-Volume 2 (pp. 1651-1655). Springer.

Bugnion, L., McArdell, B. W., Bartelt, P., and Wendeler, C. (2012). Measurements of hillslope debris flow impact pressure on obstacles. *Landslides*, 9(2), 179-187.Bugnion, L., and Wendeler, C. (2010). Shallow landslide full-scale experiments in combination with testing of a flexible barrier. *WIT Transactions on Engineering Sciences*, 67, 161-173.

Cui, Y., Choi, C. E., Liu, L. H., and Ng, C. W. (2018). Effects of particle size of mono-disperse granular flows impacting a rigid barrier. *Natural Hazards*, *91*(3), 1179-1201.

DeNatale, J. S., Iverson, R. M., Major, J. J., LaHusen, R. G., Fiegel, G. L., and Duffy, J. D. (1999). *Experimental testing of flexible barriers for containment of debris flows*. US Department of the Interior, US Geological Survey, 39p.

Eric H Y Sze, Raymond C H Koo, Jojo M Y Leung and Ken K S Ho (2018) Design of flexible barriers against sizeable landslides in Hong Kong, *HKIE Transactions*, 25:2, 115-128, DOI: 10.1080/1023697X.2018.1462107.

Hearn, G., Barrett, R. K., and Henson, H. H. (1995). Testing and modeling of two rockfall barriers. *Transportation Research Record*, 1504, 1-11.

Jakob, M., Stein, D., and Ulmi, M. (2012). Vulnerability of buildings to debris flow impact. *Natural Hazards*, 60(2), 241-261.

Kane, W. F., Fletcher, D. Q., and Duffy, J. D. (1993). Low-impact rock net testing, performance, and foundation design. In *Transportation Facilities Through Difficult Terrain. Proceedings of a Conference, Held August 8-12, 1993, Aspen-Snowmass, Colorado, USA*.

Kattel, P., Kafle, J., Fischer, J. T., Mergili, M., Tuladhar, B. M., and Pudasaini, S. P. (2018). Interaction of two-phase debris flow with obstacles. *Engineering Geology*, *242*, 197-217.

King, J. P. (2013). *Tsing Shan debris flow and debris flood (GEO Report 281*). Geotechnical Engineering Office, HKSAR, 268p.

Kwan, J. S., Chan, S. L., Cheuk, J. C., and Koo, R. C. H. (2014). A case study on an open hillside landslide impacting on a flexible rockfall barrier at Jordan Valley, Hong Kong. *Landslides,* 11(6), 1037-1050.

Leonardi, A., Wittel, F.K., Mendoza, M., Vetter, R. and Herrmann, H.J., (2016). Particle–fluid–structure interaction for debris flow impact on flexible barriers. *Computer-Aided Civil and Infrastructure Engineering,* 31(5), 323-333.

Liu, Z., Su, L., Zhang, C., Iqbal, J., Hu, B., and Dong, Z. (2020). Investigation of the dynamic process of the Xinmo landslide using the discrete element method. *Computers and Geotechnics*, 123, 103561.

Ng, C. W. W., Choi, C. E., Su, A. Y., Kwan, J. S., and Lam, C. (2016). Large-scale successive boulder impacts on a rigid barrier shielded by gabions. *Canadian Geotechnical Journal*, *53*(10), 1688-1699.

Niklaus, P., Birchler, T., Aebi, T., Schaffner, M., Cavigelli, L., Caviezel, A., Mango, M., and Benini, L. (2017). StoneNode: A low-power sensor device for induced rockfall experiments. In *2017 IEEE Sensors Applications Symposium* (SAS) (pp. 1-6). IEEE.

Park, H. S., Kim, J. Y., Kim, J. G., Choi, S. W., and Kim, Y. (2013). A new position measurement system using a motion-capture camera for wind tunnel tests. *Sensors*, 13(9), 12329-12344.

Peng, J., Fan, Z., Wu, D., Zhuang, J., Dai, F., Chen, W., and Zhao, C. (2015). Heavy rainfall triggered loess–mudstone landslide and subsequent debris flow in Tianshui, China. *Engineering Geology*, *186*, 79-90.

Platzer, K. M., Wendeler, C., Brändle, R., and Stolz, M. (2020). Experimental investigation of forces along anchors subjected to dynamic loading under tension and compression in field tests. *Canadian Geotechnical Journal*, 57(5), 770-782.

Qin, J. Q., Yin, J. H., Zhu, Z. H., and Tan, D. Y. (2020). Development and application of new FBG mini tension link transducers for monitoring dynamic response of a flexible barrier under impact loads. *Measurement*, 153, 107409.

Song, D., Choi, C. E., Ng, C. W. W., and Zhou, G. G. D. (2018). Geophysical flows impacting a flexible barrier: effects of solid-fluid interaction. *Landslides*, 15(1), 99-110.

Song, D., Zhou, G. G., Xu, M., Choi, C. E., Li, S., and Zheng, Y. (2019). Quantitative analysis of debris-flow flexible barrier capacity from momentum and energy perspectives. *Engineering Geology*, 251, 81-92.

Su, L. J., Xu, X. Q., Geng, X. Y., and Liang, S. Q. (2017). An integrated geophysical approach for investigating hydro-geological characteristics of a debris landslide in the Wenchuan earthquake area. *Engineering Geology*, 219, 52-63.

Sze, E. H., Koo, R. C., Leung, J. M., and Ho, K. K. (2018). Design of flexible barriers against sizeable landslides in Hong Kong. *HKIE Transactions*, *25*(2), 115-128.

Takahashi, T. (2014). *Debris flow: mechanics, prediction and countermeasures*. CRC press.

Tan, D. Y., Yin, J. H., Feng, W. Q., Qin, J. Q., and Zhu, Z. H. (2018a). Large-scale physical modelling study of a flexible barrier under the impact of granular flows. *Natural Hazards and Earth System Sciences,* 18, 2625-2640, https://doi.org/10.5194/nhess-18-2625-2018.

Tan, D. Y., Yin, J. H., Qin, J. Q., Zhu, Z. H., and Feng, W. Q. (2018b). Large-scale physical modeling study on the interaction between rockfall and flexible barrier. *Landslides*, 15(12), 2487-2497, https://doi.org/10.1007/s10346-018-1058-1.

Tan, D. Y., Yin, J. H., Zhu, Z. H., Qin, J. Q., and Chan, H. C. M. (2020). Fast Door-Opening Method for Quick Release of Rock Boulder or Debris in Large-Scale Physical Model. *International Journal of Geomechanics*, *20*(2), 06019019.

Volkwein, A. (2014). Flexible debris flow barriers. Design and application. *WSL Berichte. Issue 18, 29.*

Volkwein, A., and Klette, J. (2014). Semi-automatic determination of rockfall trajectories. *Sensors*, 14(10), 18187-18210.

Volkwein, A., Kummer, P., Bitnel, H., and Campana, L. (2016). Load Measurement on Foundations of Rockfall Protection Systems. *Sensors*, 16(2), 174.

Wendeler, C., Volkwein, A., McArdell, B. W., and Bartelt, P. (2019). Load model for designing flexible steel barriers for debris flow mitigation. *Canadian Geotechnical Journal*, 56: 893–910.

Wendeler, C., Volkwein, A., Roth, A., Denk, M., and Wartmann, S. (2007). Field measurements and numerical modelling of flexible debris flow barriers. *Debris flow hazards mitigation--Mechanics, prediction, and assessment*. Millpress, Rotterdam, 681-687.

Xiao, X., Su, L., Jiang, Y., Qu, X., Xu, M., Hu X., Liu Z. (2020) Experimental investigation on the impact force of the dry granular flow against a flexible barrier, *Landslides,* https://doi,org/10,1007/s10346-020-01368-9.

List of figures

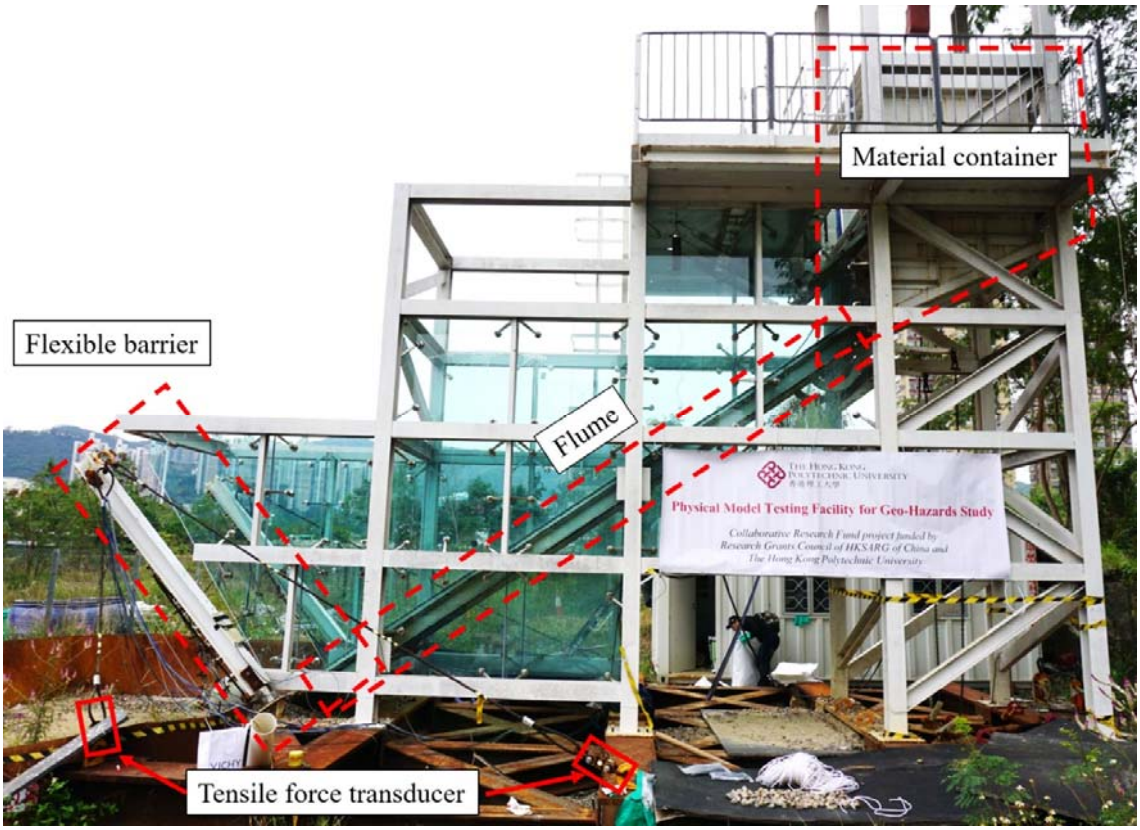

Figure 1. Side view of the large-scale physical modelling experiment facility of the Hong Kong Polytechnic University

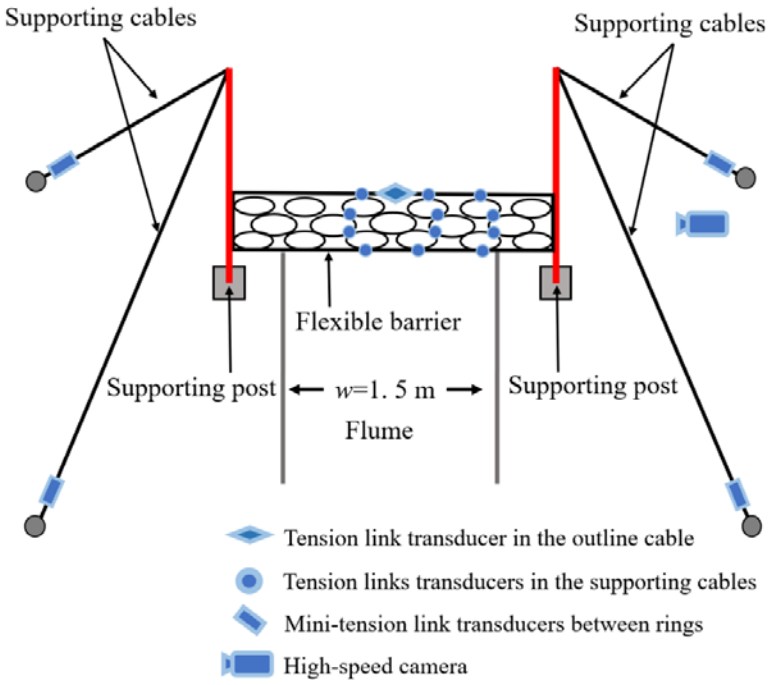

Figure 2. Instrumentation arrangement in the large-scale physical modelling experiment facility

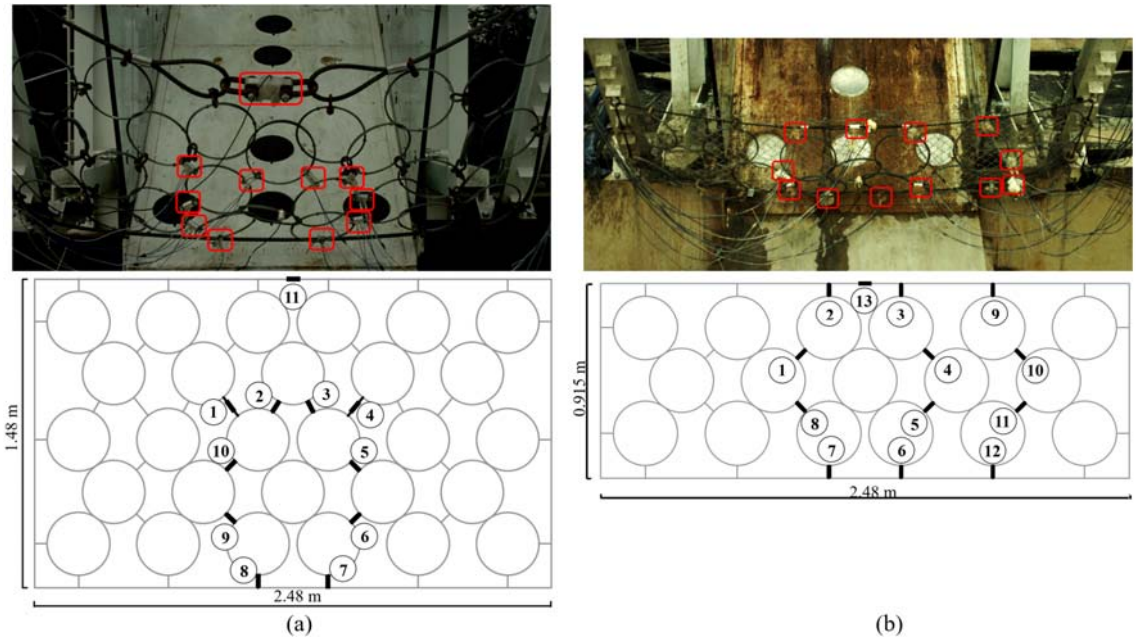

Figure 3. Arrangement of the mini-tension link transducers in the flexible nets for (a) boulder impact tests and (b) debris flow impact test

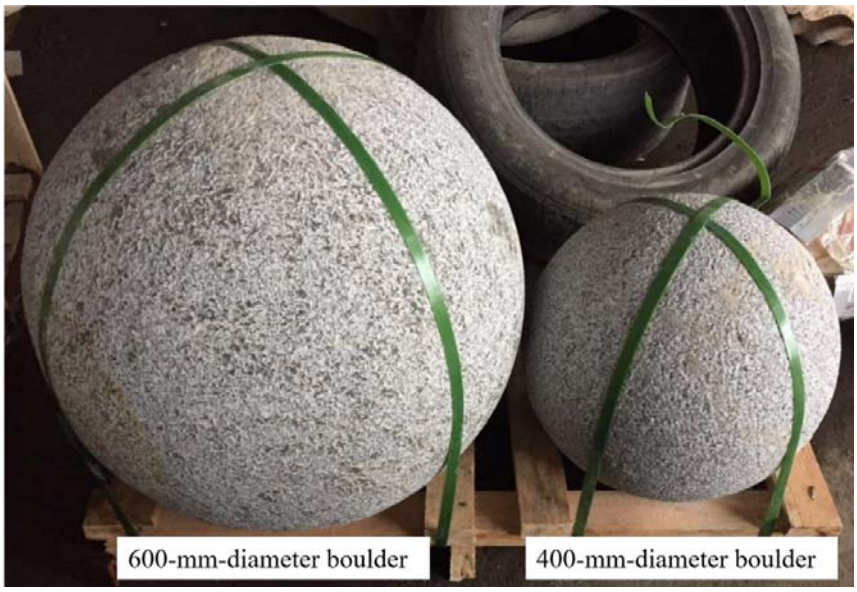

(a)

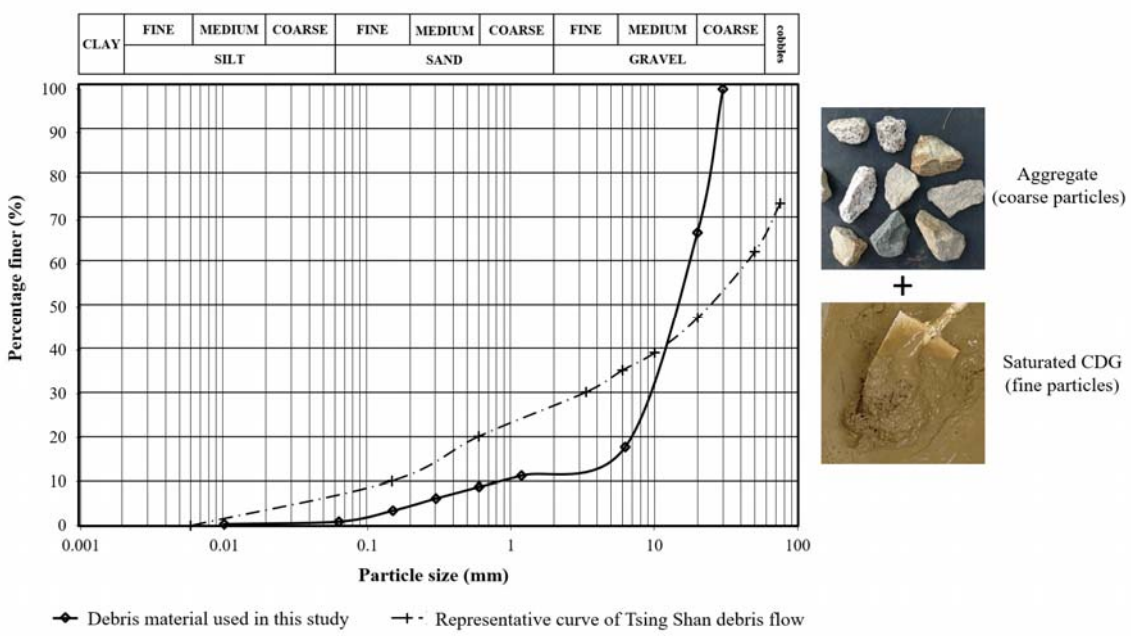

(b)

Figure 4. (a) Granite boulders and (b) composition and particle size distribution (PSD) of the debris material used in this study

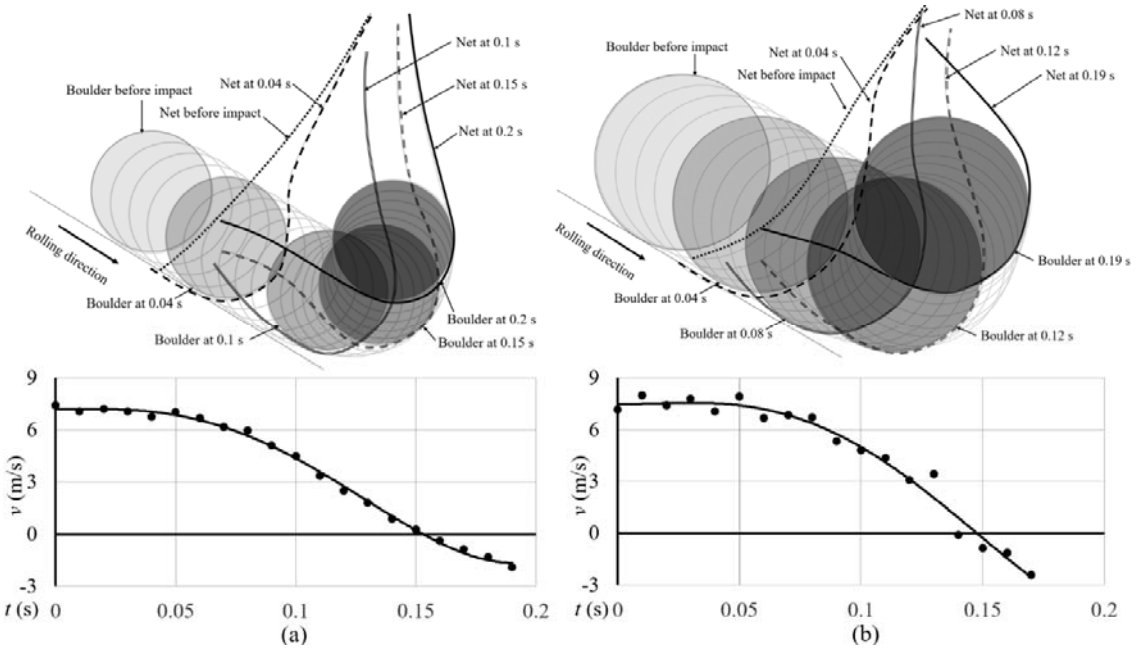

Figure 5. Movement trajectory of the boulder and velocity component in the impact direction *v.s.* time in the (a) 400-mm and (b) 600-mm boulder impact tests

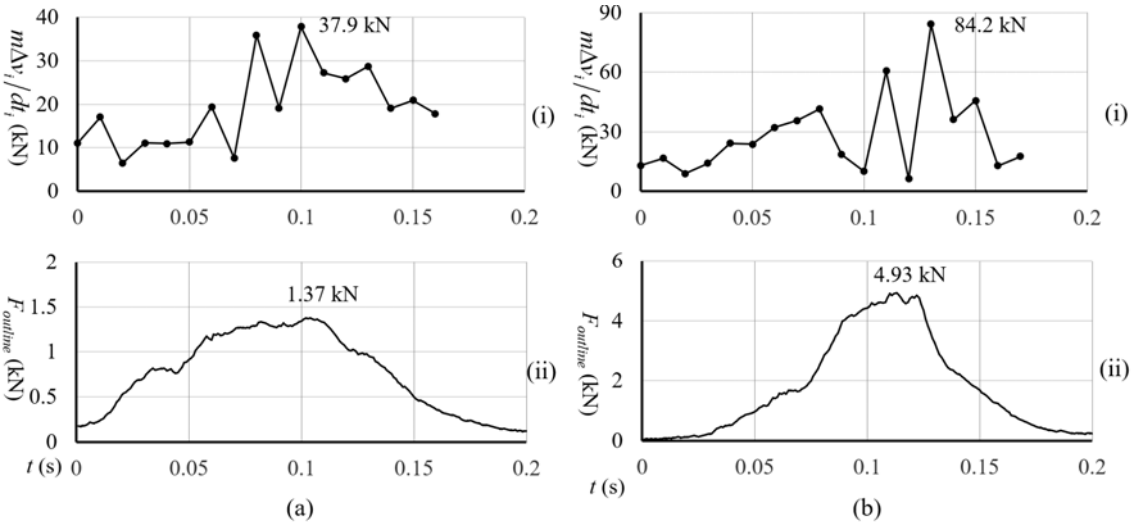

Figure 6. (i) Impact force induced by the boulder and (ii) tensile force in the outline cable in the (a) 400-mm and (b) 600-mm boulder impact tests

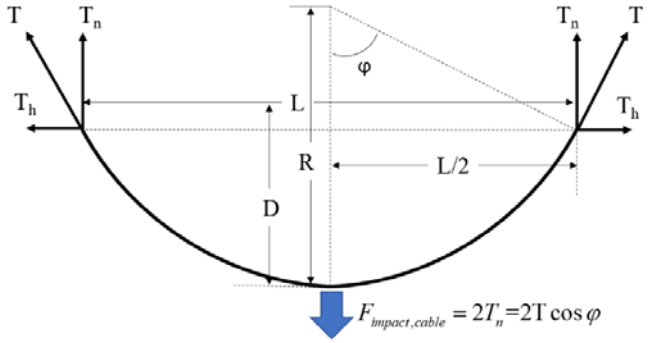

Figure 7. Decomposing of the tensile force in a horizontal cable

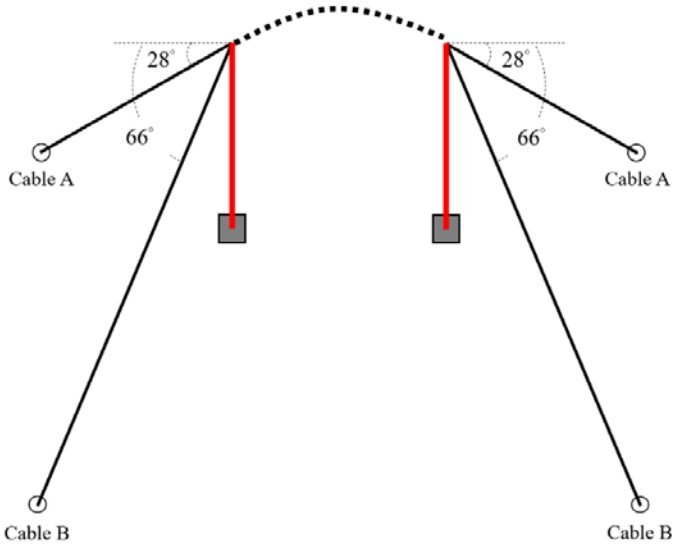

(a)

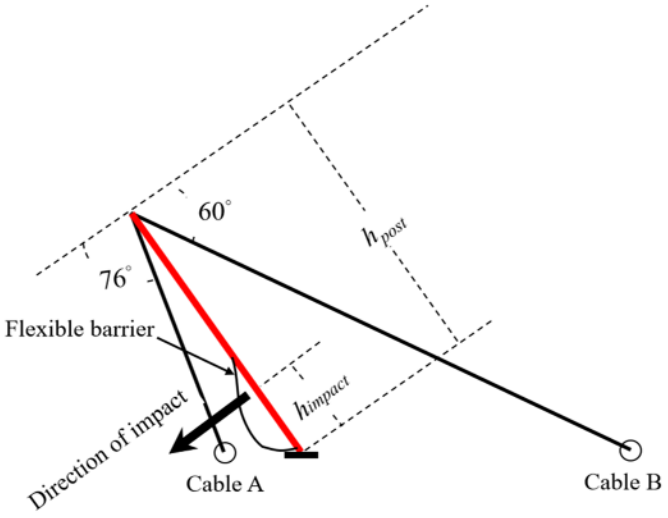

(b)

Figure 8. (a) Top view and (b) side view of the arrangement of the supporting structures of the studied flexible barrier

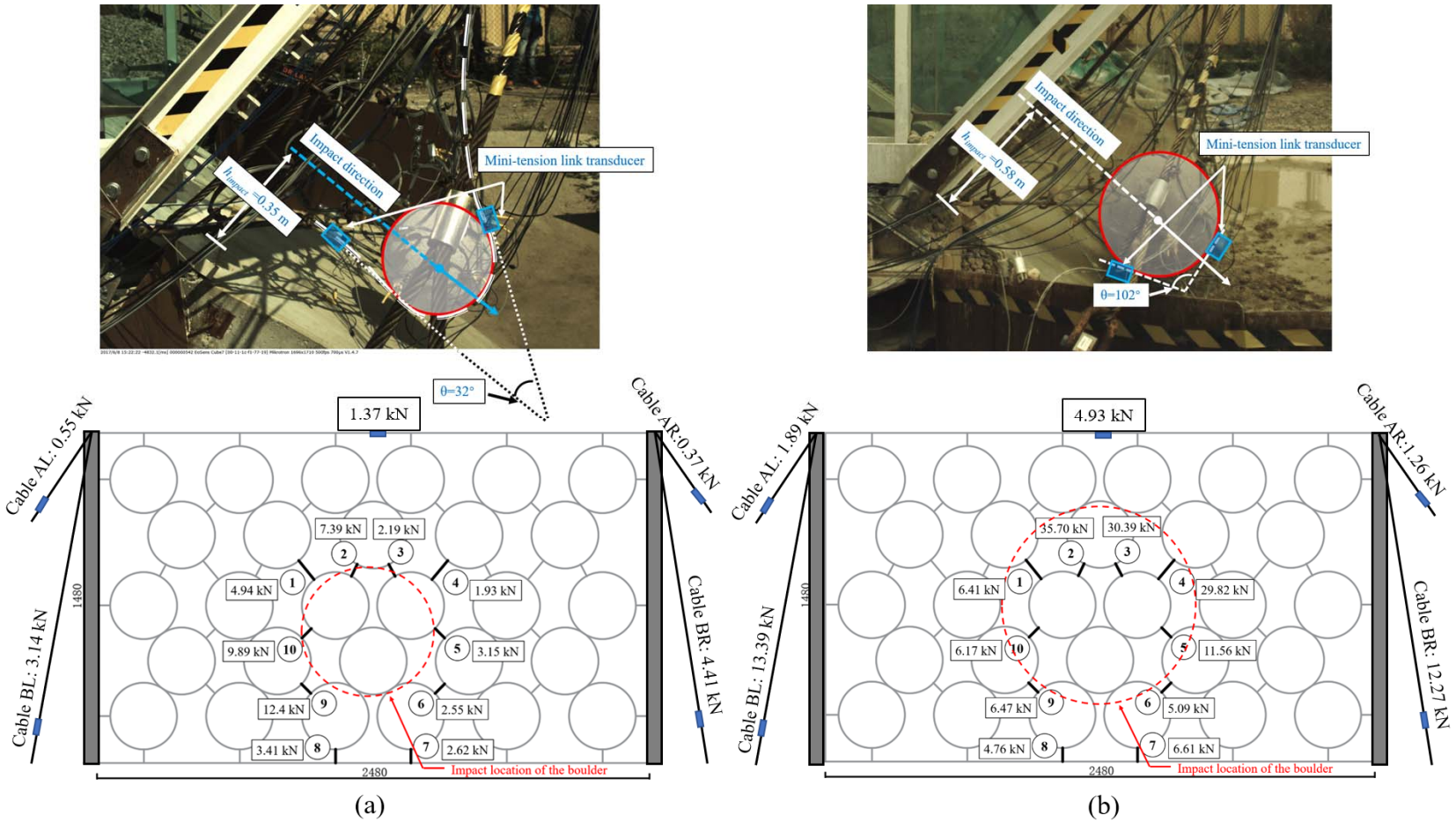

Figure 9. Photograph of the transducers in the flexible barrier at the largest deformation and the peak forces in (a) 400-mm and (b) 600-mm boulder impact tests

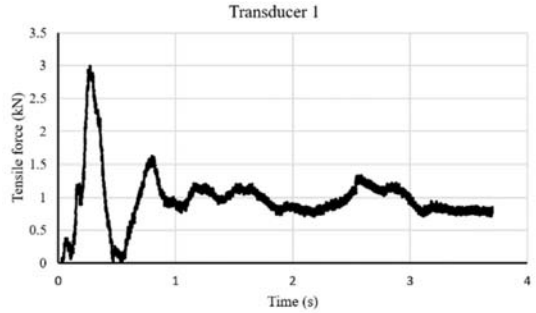
Transducer 1
Tensile force (kN)
Time (s)

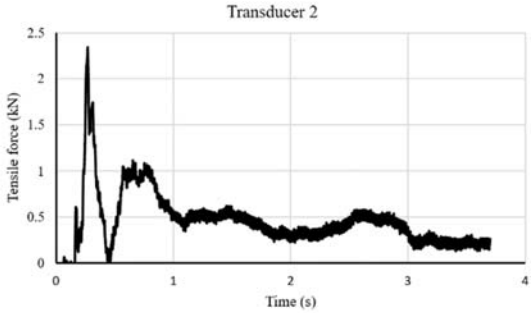
Transducer 2
Tensile force (kN)
Time (s)

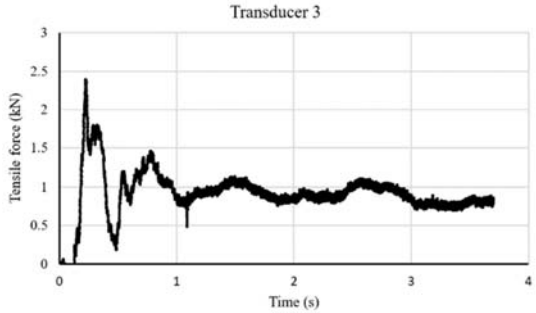
Transducer 3
Tensile force (kN)
Time (s)

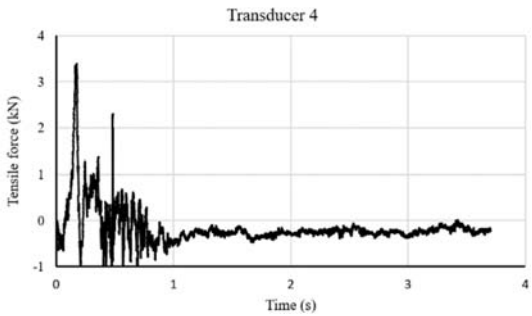
Transducer 4
Tensile force (kN)
Time (s)

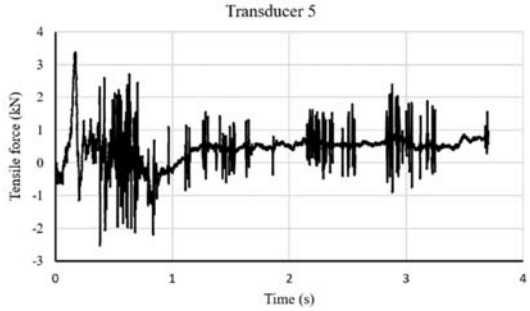
Transducer 5
Tensile force (kN)
Time (s)

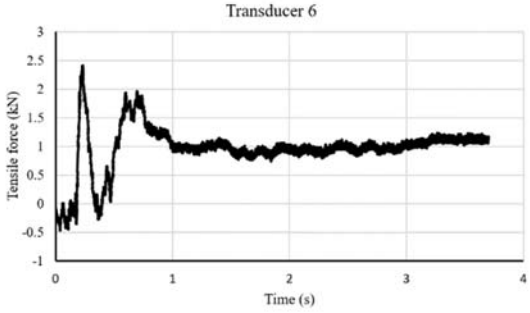
Transducer 6
Tensile force (kN)
Time (s)

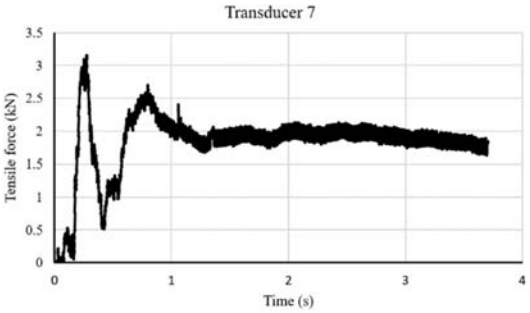
Transducer 7
Tensile force (kN)
Time (s)

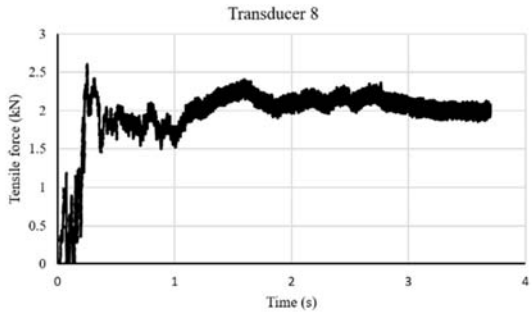
Transducer 8
Tensile force (kN)
Time (s)

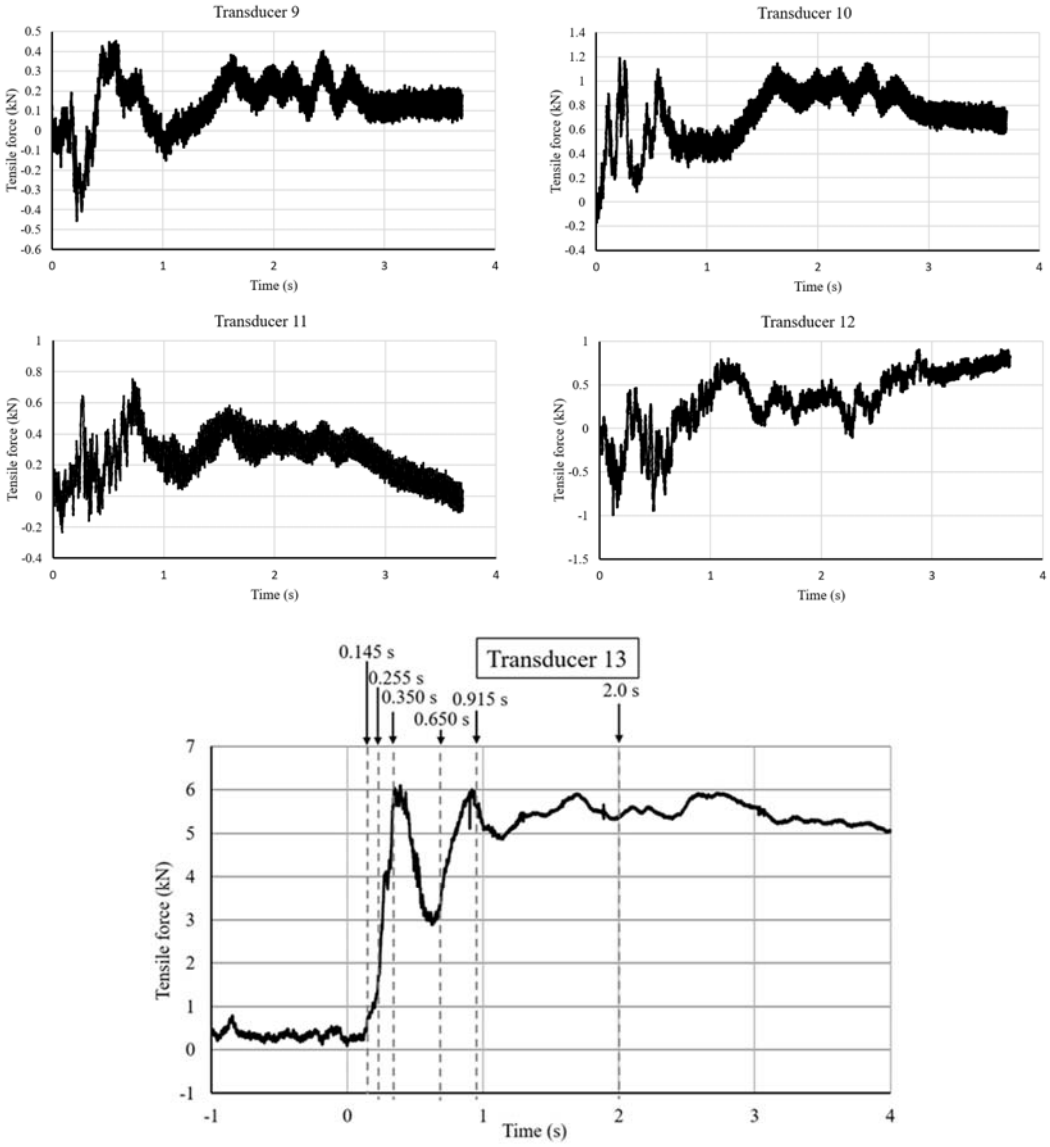

Figure 10. Forces of the tension link transducers installed in the flexible net in the debris flow test

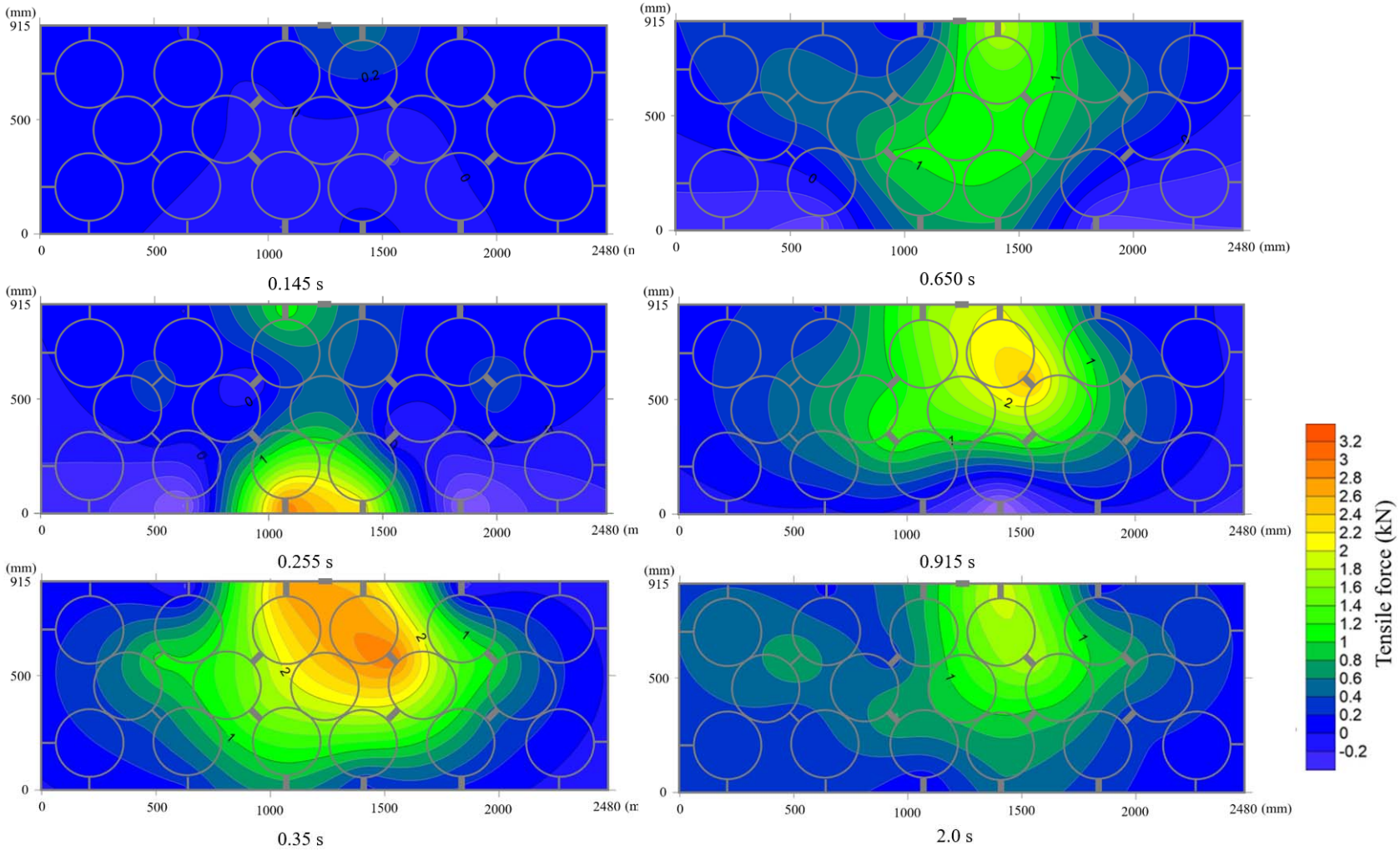

Figure 11. Distribution of the pressure induced by a debris flow at typical times since initial impact

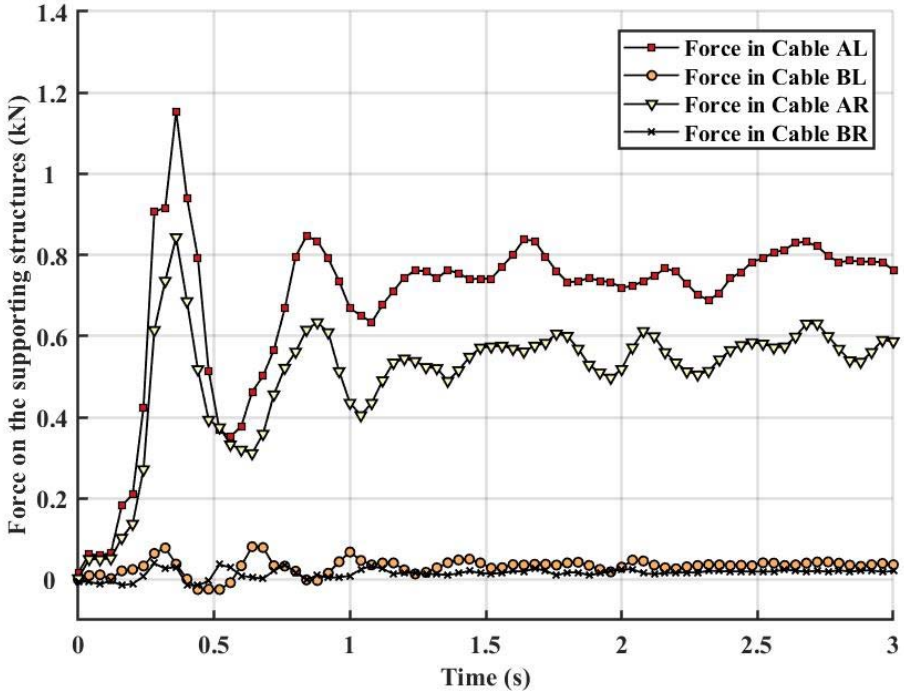

Figure 12. Tensile forces in the supporting cables in the debris flow impact test

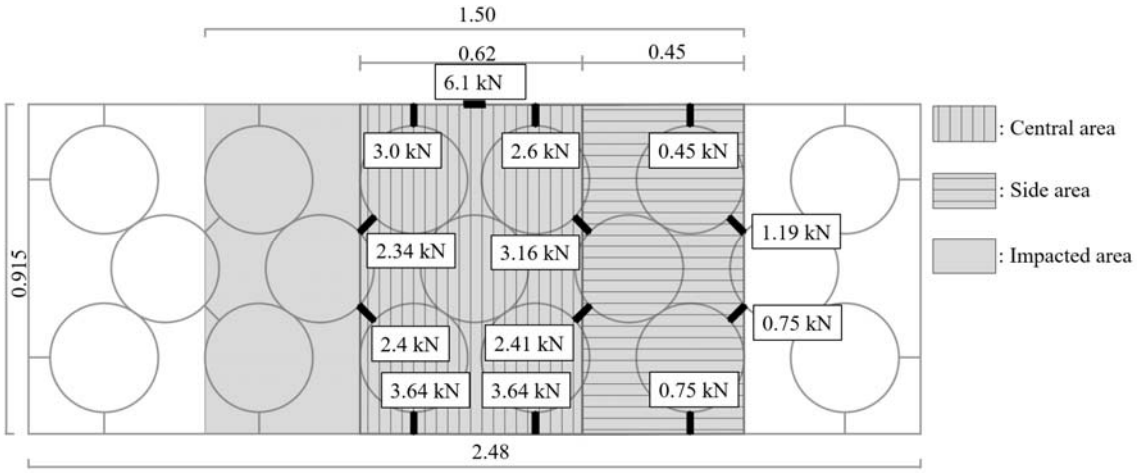

(a)

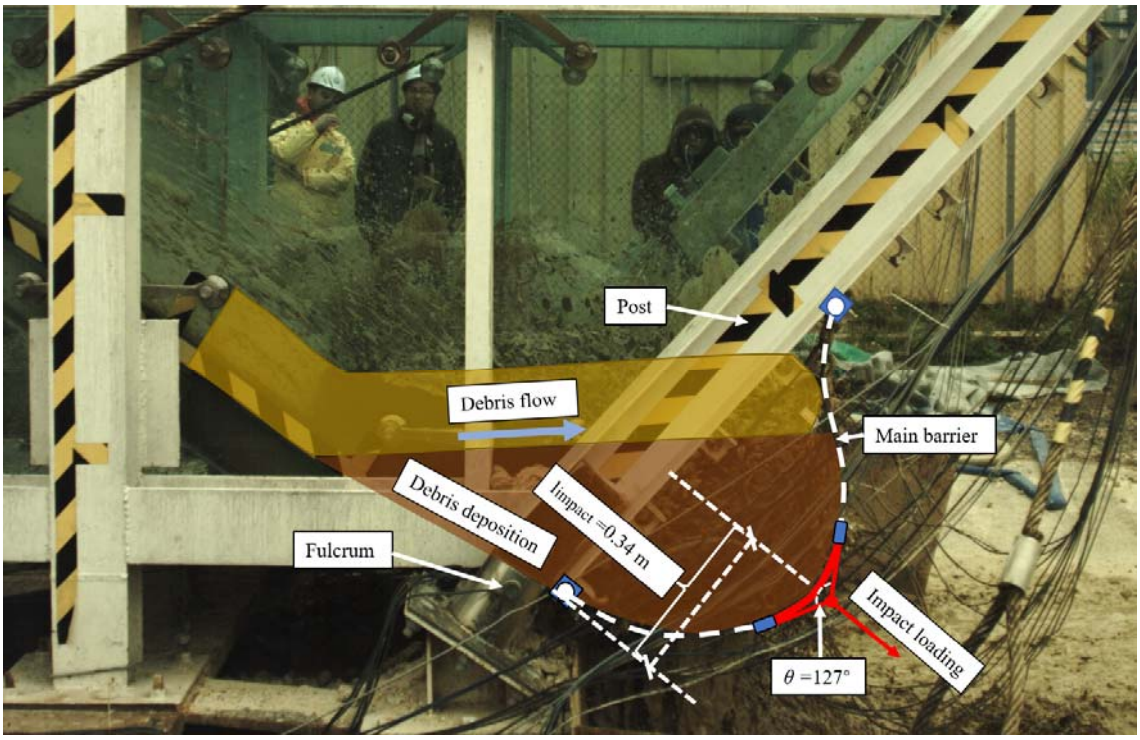

(b)

Figure 13. (a) Peak forces of the mini tension link transducers in the flexible barrier and (b) photograph of the flexible barrier at the largest deformation in the debris flow test

12 Table 1. Verification of the methods for measuring impact forces in the boulder impact tests

	Description of the method	400-mm boulder impact test		600-mm boulder impact test	
		Impact force (kN)	**Relative error**	**Impact force (kN)**	**Relative error**
Back-calculated impact force	$F_i = \frac{m \cdot \Delta v_i}{dt_i}$ momentum conservation law	37.9	N/A	84.2	N/A
Methods for impact force measurement	$F_{impact,cable} = \sum_{i=1}^{n} 2T_i \cos\varphi_i$ proposed by Song *et al.* (2017)	5.48	-85.5%	19.72	-76.6%
	Analytical solution for impact force on the supporting structures	25.8	-31.9%	52.9	-37.2%
	$F_{impact,net} = \cos\frac{\theta}{2}\sum_{i=1}^{n} T'_{ring,i}$ proposed by Tan *et al.* (2018a)	37.9	0	72.4	-14%

13

14

15 Table 2. Verification of the methods for measuring impact force in the debris flow impact test

Methods for impact force measurement	Calculated impact force (kN)	Relative error comparing with the impact force on the net
$F_{impact,net} = \cos\frac{\theta}{2}\sum_{i=1}^{n} T'_{ring,i}$ Impact force on the net	10.35	N/A
Impact force on the supporting structures	7.1	-31.4%
$F_{impact,outline} = \sum_{i=1}^{n} 2T_i \cos\varphi_i$ (uniform impact load distribution)	24.4	+135.7%
$F_{impact,outline} = \frac{1}{2}\sum_{i=1}^{n} 2T_i \cos\varphi_i$ (triangular impact load distribution)	12.2	+17.9%

16

17